Supporting Information

Huber and Lindner 10.1073/pnas.1110813108

SI Text

Vortex Translation Operators. In the following, we derive the commutation relations for the vortex translation operators

$$\mathcal{T}_x\mathcal{T}_y = \mathcal{T}_y\mathcal{T}_x \exp(2\pi i\hat{N}_b/N), \qquad \text{[S1]}$$

and discuss their relation to the vortex Barry phase. Our derivation of Eq. **S1** holds for any interaction strength U in the Bose Hubbard model (Eq. **5**). We consider the Hamiltonian of Eq. **5** on a torus with $N = L_xL_y$ sites. The gauge field $A_{\mathbf{rr}'}$ describes one flux quantum piercing the surface of the torus uniformly, whereby the flux per plaquette is given by

$$B = \frac{2\pi}{L_xL_y}. \qquad \text{[S2]}$$

An important gauge invariant quantity described by the gauge field $\mathbf{A}$ is the Wilson loop functions

$$\Phi_x(y) = \oint dx A_x, \qquad \Phi_y(x) = \oint dy A_y. \qquad \text{[S3]}$$

We choose a continuous parametrization of the gauge field, which yields a continuous family of Wilson line function. Our gauge choice is given by

$$A^x_{\mathbf{r},\mathbf{r}+\hat{x}} = yBL_x\delta_{x,L_x-1} + \frac{\Theta_y}{L_x} \qquad A^y_{\mathbf{r},\mathbf{r}+\hat{y}} = xBL_x + \frac{\Theta_x}{L_y}, \qquad \text{[S4]}$$

where $x = 0,\ldots,L_x - 1$, and $y = 0,\ldots,L_y - 1$. Our gauge choice is shown in Fig. S1. The two Wilson loop functions are given by

$$\Phi_y(x) = xBL_y + \Theta_y, \qquad \text{[S5]}$$

$$\Phi_x(y) = -yBL_x + \Theta_x. \qquad \text{[S6]}$$

Note that the parameters $\Theta_x,\Theta_y \in [0,2\pi]$ define a *continuous* family of Hamiltonians, which are *inequivalent* under gauge transformation.

Let t_x and t_y be lattice translation operators, i.e.,

$$t_x^\dagger b_{\mathbf{r}} t_x = b_{\mathbf{r}+\hat{\mathbf{x}}}, \qquad t_y^\dagger b_{\mathbf{r}} t_y = b_{\mathbf{r}+\hat{\mathbf{y}}}. \qquad \text{[S7]}$$

Translating the Hamiltonian by t_x and t_y leads to

$$t_\alpha^\dagger \mathcal{H}[\mathbf{A}]t_\alpha = \mathcal{H}[\tilde{\mathbf{A}}^{(\alpha)}], \qquad \tilde{\mathbf{A}}^{(\alpha)}_{\mathbf{r},\mathbf{r}'} = A_{t_\alpha^{-1}(\mathbf{r}),t_\alpha^{-1}(\mathbf{r}')}. \qquad \text{[8]}$$

The gauge invariant content of the new gauge fields $\tilde{\mathbf{A}}^{(\alpha)}$ is the same flux per plaquette B as for $\mathbf{A}$, however, the Wilson line functions of Eq. **S3** are shifted by one lattice constant,

$$t_x\colon \Phi_y(x) \to \tilde{\Phi}_y(x) = \Phi_y(x-1) \qquad t_y\colon \Phi_x(y) \to \tilde{\Phi}_x(y) = \Phi_x(y-1). \qquad \text{[S9]}$$

Note that the values of the Wilson lines cannot be changed by a gauge transformation. Therefore, if we conjugate the Hamiltonian by t_x or t_y, we cannot make a gauge transformation back to the original Hamiltonian. However, we can find gauge transformations U_x and U_y that yield the following relations:

$$U_\alpha^\dagger t_\alpha^\dagger \mathcal{H}[\mathbf{A}(\boldsymbol{\Theta})]t_\alpha U_\alpha = \mathcal{H}[\mathbf{A}(\boldsymbol{\Theta} - \Delta\boldsymbol{\Theta}^{(\alpha)})], \qquad \text{[S10]}$$

where $\boldsymbol{\Theta} = (\Theta_x,\Theta_y)$, and

$$(\Delta\boldsymbol{\Theta}^{(\alpha)})_\beta = \epsilon^{\alpha\beta}BL_\beta, \qquad \text{[S11]}$$

where $\epsilon^{\alpha\beta}$ is an antisymmetric tensor with $\epsilon^{xy} = 1$.

We parametrize the unitaries U_x and U_y as

$$U_x = \exp\left(i2\pi\sum_{\mathbf{r}}\chi^x_{\mathbf{r}}b^\dagger_{\mathbf{r}}b_{\mathbf{r}}\right), \quad U_y = \exp\left(i2\pi\sum_{\mathbf{r}}\chi^y_{\mathbf{r}}b^\dagger_{\mathbf{r}}b_{\mathbf{r}}\right),$$

where the functions $\chi^\alpha_{\mathbf{r}}$ are given by

$$\chi^\alpha_{\mathbf{r}} = \int^{\mathbf{r}} d\mathbf{r}' \cdot [\mathbf{A}(\boldsymbol{\Theta} - \Delta\boldsymbol{\Theta}^{(\alpha)}) - \tilde{\mathbf{A}}^{(\alpha)}]. \qquad \text{[S12]}$$

We now calculate the commutation relation between $\mathcal{T}_x$ and $\mathcal{T}_y$. An explicit formula for $\chi^\alpha_{\mathbf{r}}$ using the gauge choice Eq. **S4** reads

$$\chi^x(\mathbf{r}) = -BL_xy\delta_{x,0}, \qquad \chi^y(\mathbf{r}) = Bx. \qquad \text{[S13]}$$

Multiplying these operators, we get

$$\mathcal{T}_y\mathcal{T}_x = t_yt_x \exp\left(i\sum_{\mathbf{r}}(\chi^x_{\mathbf{r}} + \chi^y_{\mathbf{r}-x})b^\dagger_{\mathbf{r}}b_{\mathbf{r}}\right),$$

$$\mathcal{T}_x\mathcal{T}_y = t_xt_y \exp\left(i\sum_{\mathbf{r}}(\chi^x_{\mathbf{r}-y} + \chi^y_{\mathbf{r}})b^\dagger_{\mathbf{r}}b_{\mathbf{r}}\right) = \mathcal{T}_y\mathcal{T}_x \exp(i\Upsilon). \qquad \text{[S14]}$$

In the above equation, we have used $[t_x,t_y] = 0$. The factor $\exp(i\Upsilon)$ is given by

$$\Upsilon = -\sum_{\mathbf{r}}\omega_{\mathbf{r}}b^\dagger_{\mathbf{r}}b_{\mathbf{r}}, \qquad \text{[15]}$$

with

$$\omega_{\mathbf{r}} = \chi^x_{\mathbf{r}} - \chi^x_{\mathbf{r}-\mathbf{y}} + \chi^y_{\mathbf{r}-\mathbf{x}} - \chi^y_{\mathbf{r}}. \qquad \text{[S16]}$$

Using Eq. **S13** we get

$$\omega_{\mathbf{r}} = -B, \qquad \text{[S17]}$$

and substituting this into Eq. **S14**, we arrive at our final result

$$\mathcal{T}_x\mathcal{T}_y = \mathcal{T}_y\mathcal{T}_x \exp(2\pi i\hat{N}_b/N). \qquad \text{[S18]}$$

Here, $\hat{N}_b$ is the boson number operator and N are the number of sites.

Note that, although explicit gauge choices were made in the derivation of Eq. **S4**, the result is gauge invariant: A different gauge choice in Eq. **S1** yields the same result.

To relate $\mathcal{T}_x$ and $\mathcal{T}_y$ to the vortex position, we note that the vortex position can only depend on the values of the Wilson lines $\Phi_x(y)$ and $\Phi_y(x)$, because these are the only gauge invariant quantities that break the translational symmetry on the torus. Therefore, the ground states of the continuous family of Hamiltonians $\mathcal{H}[\mathbf{A}(\boldsymbol{\Theta})]$ correspond to many body states $\Psi(\boldsymbol{\Theta})$ with vortex positions continuously parametrized by $\boldsymbol{\Theta}$ as well. The vortex

position in the many body states $\Psi(\mathbf{\Theta})$ has quantum fluctuations; the amplitudes, however, are centered around a point $\mathbf{R}_V$, which depends only on $\mathbf{\Theta}$ (see refs. 1 and 2). As a result, the action of $\mathcal{T}_x$ and $\mathcal{T}_y$ shifts the vortex position by one lattice site in the x and y direction accordingly.

To relate Eq. **S18** to $2\pi\alpha$, the Berry phase acquired by moving a vortex around a dual lattice plaquette, we note that

$$\exp(i2\pi\alpha) = \exp\left(i\oint d\Theta_\mu \mathcal{A}_\mu\right) = \langle\Psi(\mathbf{\Theta}^0)|U_4U_3U_2U_1|\Psi(\mathbf{\Theta}^0)\rangle, \quad \textbf{[S19]}$$

where $\mathcal{A}_\mu = i\langle\Psi(\mathbf{\Theta})|\partial_{\Theta_\mu}\Psi(\mathbf{\Theta})\rangle$, and the line integral is taken around a plaquette in flux space of size (BL_y,BL_x). In Eq. **S19**, $U_i = U(\mathbf{\Theta}^i,\mathbf{\Theta}^{i+1})$ are adiabatic evolution operators from $\mathbf{\Theta}^i$ to $\mathbf{\Theta}^{i+1}$, and

$$\begin{aligned}\mathbf{\Theta}^1 &= \mathbf{\Theta}^0 + \Delta\mathbf{\Theta}^{(x)}\mathbf{\Theta}^2 = \mathbf{\Theta}^0 + \Delta\mathbf{\Theta}^{(x)} + \Delta\mathbf{\Theta}^{(y)}\mathbf{\Theta}^3\\ &= \mathbf{\Theta}^0 + \Delta\mathbf{\Theta}^{(y)}\mathbf{\Theta}^4 = \mathbf{\Theta}^0. \quad \textbf{[20]}\end{aligned}$$

Using $U_3 = \mathcal{T}_y U_1^\dagger \mathcal{T}_y^\dagger$ and $U_4 = \mathcal{T}_x^\dagger U_2^\dagger \mathcal{T}_x$, and assuming that the ground state $|\Psi(\mathbf{\Theta})\rangle$ is nondegenerate, we find

$$\begin{aligned}\exp\left(i\oint d\Theta_\mu \mathcal{A}_\mu\right) &= \langle\Psi(\mathbf{\Theta}^0)|\mathcal{T}_y^\dagger\mathcal{T}_x^\dagger\mathcal{T}_y\mathcal{T}_x|\Psi(\mathbf{\Theta}^0)\rangle\\ &= \exp(-i2\pi n_b). \quad \textbf{[S21]}\end{aligned}$$

Finally, from Eq. **S21**, we see that the Berry flux through an elementary plaquette in flux space (which has the topology of a torus) is $2\pi(n_b + p)$. All of the N elementary plaquette on the flux torus are identical. The Hall conductivity is given by the integral of the Berry curvature on the whole flux torus (3) and, therefore, in the presence of one vortex,

$$\sigma_{xy} = N(n_b + p). \quad \textbf{[S22]}$$

Vortex Hopping Hamiltonian. In the following, we derive the form of the effective vortex Hamiltonian (Eq. **25**). Let us start with the terms arising from a change in the Aharonov–Bohm (AB) fluxes $\mathbf{\Theta} = \mathbf{\Theta}^0 + \Delta\mathbf{\Theta}$, which moves the minimum of the vortex potential $U(\mathbf{R} - \mathbf{R}_V)$ according to Eq. **24**. We can now apply degenerate perturbation theory in the subspace of $|R\rangle$ and $|L\rangle$. The effect of $\Delta\mathbf{\Theta}$ only leads to off-diagonal matrix elements between $|R\rangle$ and $|L\rangle$ because both states have the same $|\psi(\mathbf{R} - \mathbf{R}_V)|$ and the perturbation is diagonal with respect to $\mathbf{R}$. The state $|R\rangle + e^{-i\varphi}|L\rangle$ has excess weight along $\arctan(x/y) = \varphi$, and therefore becomes the ground state for $\Delta\mathbf{R}_V$ along that direction, i.e.,

$$\mathcal{H}_V = \tilde{U}(-\Delta\Theta_y\sigma_x + \Delta\Theta_x\sigma_y). \quad \textbf{[S23]}$$

We now consider the effect of the particle-hole symmetry (PHS) breaking terms of Eq. **19**. We expect the two ground states $|R\rangle$ and $|L\rangle$ to conform to two charge density wave orders centered at $\mathbf{R}_V$ because the moving vortex exerts a force on the particles due to the Josephson relation. We note that the two charge density wave orders decay exponentially with the distance from $\mathbf{R}_V$ (the decay length scale is the lattice constant) (1, 2). To see which of the states ($|R\rangle$ or $|L\rangle$) has an excess (reduced) density at $\mathbf{R}_V$, we consider an analogy with a particle hopping on a ring around $\mathbf{R}_V$.

In Fig. S2, we show the energy of a particle on a ring for the two states $|R\rangle$ with $m = 0$ and $|L\rangle$ with $m = 1$ as a function of the flux Φ_D through the center of the ring. Note that the energy of $|R\rangle$ for $\Phi_D = \pi - \delta$ is equal to that of $|L\rangle$ for $\Phi_D = \pi + \delta$ (at $\Phi_D = \pi$ the two states are degenerate). Consider now the vortex Hamiltonian of Eq. **23**. At half-filling for hard-core bosons (HCBs), we can consider two dual flux configurations, which at R_V have $\Phi_D(\mathbf{R}_V) = \pi \pm \delta$. Via $\Phi_D(\mathbf{r}) = 2\pi\langle S^z_{\mathbf{r}} + \frac{1}{2}\rangle$, they are related to two corresponding charge configurations (the two configurations are related by charge conjugation). From the analogy to the particle on a ring, we can infer that these two charge configurations lead to the vortex ground states $|L\rangle$, $|R\rangle$, respectively. We therefore conclude that the state $|L\rangle$ ($|R\rangle$) has an excess (reduced) density at $\mathbf{R}_V$, respectively (see Fig. S2).

Whereas for the particle-hole symmetric point, these charge configurations are equivalent energetically, the assisted hopping (t^2/U) terms in Eq. **19** give different energies for the two configurations. Due to the exponential decay of the charge density wave order (1, 2), the difference between the expectation value of these terms in the states $|L\rangle$, $|R\rangle$ is also going to decay exponentially with the distance to $\mathbf{R}_V$.

To account for their effect, we estimate the energy change using mean-field HCBs states for $|L\rangle$, $|R\rangle$ of the form $|\Psi\rangle = \prod_{\mathbf{r}}|\psi_{\mathbf{r}}(\vartheta_{\mathbf{r}})\rangle$, with

$$|\psi(\vartheta_{\mathbf{r}})\rangle = \cos(\vartheta_{\mathbf{r}})|\downarrow\rangle + \sin(\vartheta_{\mathbf{r}})e^{i\varphi_{\mathbf{r}}}|\uparrow\rangle. \quad \textbf{[S24]}$$

Here $\varphi_{\mathbf{r}}$ is the phase arising due to the vortex. Because of the exponential decay of the charge density wave order, we only consider the 3×3 cluster shown in Fig. S2. We evaluate the assisted hopping (Eq. **19**) in a state where the parameters ϑ_r are chosen such that the center site has $n_b = \frac{1}{2} \pm \delta$, its nearest neighbors $n_b = \frac{1}{2} \mp \delta/4$, and the sites at the corners of the cluster have $n_b = \frac{1}{2}$. We find that the energy difference is dominated by assisted hopping terms that hop over the central site $\mathbf{R}_V$

$$\begin{aligned}E(|L\rangle) - E(|R\rangle) \approx -\varepsilon_m \sum_{\mathbf{r},\mathbf{r}'}\Bigg[&\left\langle L|e^{iA_{\mathbf{r}\mathbf{r}'}}S^+_{\mathbf{r}}\left(S^z_{\mathbf{R}_V} + \frac{1}{2}\right)S^-_{\mathbf{r}'}|L\right\rangle\\ &- \left\langle R|e^{iA_{\mathbf{r}\mathbf{r}'}}S^+_{\mathbf{r}}\left(S^z_{\mathbf{R}_V} + \frac{1}{2}\right)S^-_{\mathbf{r}'}|R\right\rangle\Bigg], \quad \textbf{[S25]}\end{aligned}$$

where $\mathbf{r}$ and $\mathbf{r}'$ are nearest neighbors of $\mathbf{R}_V$. As discussed above, the state $|L\rangle$ corresponds to higher density at $\mathbf{R}_V$, therefore, the quantity above is negative.

The combined effect of moving the vortex position $\mathbf{R}_V$ away from a direct lattice site and the PHS breaking terms of [**19**] leads to the low-energy effective Hamiltonian near the degeneracy point

$$\mathcal{H}_V = \tilde{U}(-\Delta\Theta_y\sigma_x + \Delta\Theta_x\sigma_y) + \tilde{\epsilon}\sigma_z, \quad \textbf{[S26]}$$

which is given in Eq. **25**.

Exact Diagonalization. We calculate the ground-state wave function for different AB fluxes using the Algorithms and Libraries for Physics Simulations Lanczos application (4) on a 3×3 cluster. We choose the same gauge choice as depicted in Fig. S1. To obtain the phase diagram, we truncate the local Hilbert space to include all occupation states up to five particles per site.

To get some insight into finite size effects, we also calculate σ_{xy} for a 3×4 cluster at filling $n_b = 1$. To compare the two cluster sizes, we estimate the Mott transition by considering the gap to the first excited state. We attribute the transition to a kink in the gap as a function of t/U. If we rescale the results for the Hall conductivity by the critical t/U, the change from $\sigma_{xy} = 0$ to $\sigma_{xy} = 1$ obtained with the two clusters fall on top of each other.

1. NH Lindner, A Auerbach, DP Arovas (2009) Vortex quantum dynamics of two dimensional lattice bosons. *Phys Rev Lett* 102:070403.
2. N Lindner, A Auerbach, DP Arovas (2010) Vortex dynamics and Hall conductivity of hard core bosons. *Phys Rev B Condens Matter Mater Phys* 82:134510.
3. JE Avron, R Seiler (1985) Quantization of the Hall conductance for general, multiparticle Schrödinger Hamiltonians. *Phys Rev Lett* 54:259–262.
4. AF Albuquerque, et al. (2007) The ALPS project release 1.3: Open-source software for strongly correlated systems. *J Magn Magn Mater* 310:1187–1193.

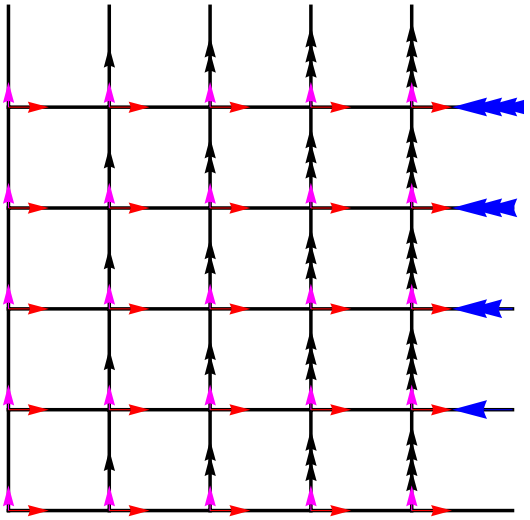

Fig. S1. The gauge choice Eq. **S4**. Arrows on links represent the values for $A_{r,r'}$: Black arrows represent a value of B; blue arrows represent BL_x; red represent Θ_x/L_x; and magenta Θ_y/L_y. Open links stand for periodic boundary conditions.

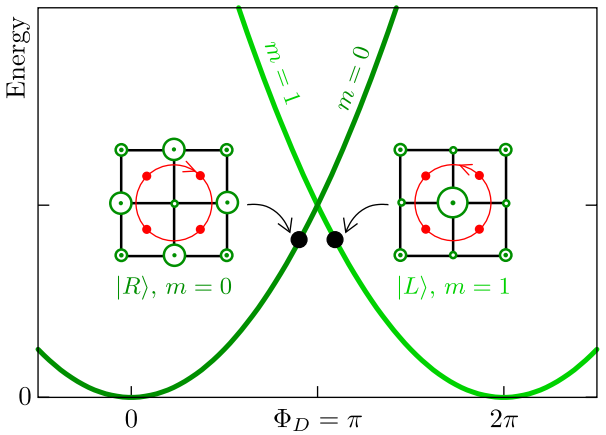

Fig. S2. Vortex Hamiltonian. The green curves show the energy for a particle on a ring as a function of the flux through its center. At slightly higher (lower) flux than $\Phi_D = \pi$, the state $m = 1$ ($m = 0$) is the ground state. Two charge density waves centered at $\mathbf{R}_V$ lead to $\Phi_D = \pi + \delta, \pi - \delta$ and correspond to the states $|L\rangle$, $|R\rangle$, which have the same energy. Therefore, the state $|L\rangle$ ($m = 1$) corresponds to a charge density wave with excess density at the center site.